Scholarly Research Journal for Interdisciplinary Studies,
Online ISSN 2278-8808, SJIF 2016 = 6.177, www.srjis.com
UGC Approved Sr. No.49366, JULY-AUG 2017, VOL- 4/35

A STUDY ON ANTIMICROBIAL ACTIVITY OF CERIUM OXIDE NANOPARTICALS PREPARED FROM MORINGA OLEIFERA

Kanumalla Raghu Kranti Kumar
Lecturer in Zoology, Dept of Zoology, Sri Vivekananda Degree College, Podili, A.P

1. Introduction: Cerium oxide is a material semiconductor with wide energy band gap of 3.19 eV and a wavelength of 330–370 nm . It has a unique chemical and thermal stability, high conductivity, reliable oxygen storage, ability to adsorb UV light, and catalytic activity.Due these advantageous properties, cerium oxide has been heavily utilized in various fields of application, i.e., UV light absorbers , glass polishing, biosensors, cosmetics as sun screen lotion , and biomedical applications . The most extensively utilized approach for fabricating nano-sized particles is green metal and metal oxide synthesis. Among the common approaches is the use of plant extracts, primarily due to their abundant availability in nature, by the utilization of their secondary metabolite. These secondary metabolites act as natural reducing and capping agents, and hence are environmentally-friendly and less toxic when applied in the biomedical, pharmacology, and cosmetic industries. In addition, this method can be scaled up to industry level.

The use of plant extracts in the synthesis has been described in a number of publications to synthesis of CeO_2NPs, such as *Gloriosa superba* leaf extract , *Acalypha indica* leaf extract, *Aloe vera*, *Hibiscus sabdarifa* flower extract , *Olei europaea* leaf extract , *Sida acuta* leaf extract, *Prosofis julifora* leaf extract, and *Calotropis procera* flower extract. In this work, the synthesis of CeO_2NPs was carried out using *Moringa oleifera* leaf extract. Based on related literature, there are no studies on the synthesis of CeO_2NPs using *M. oleifera* leaf extract.

In this research, green synthesis was carried out by a precipitation method because of its simplicity, relatively low cost, and reaction in low temperature

2. Material and methods

2.1. Materials and reagents: Cerium nitrate hexahydrate ($Ce(NO_3)_3{\cdot}6H_2O$, 99.5), *chitosan medium molecular weight*, 75–85% *deacetylated*, Montmorillonite K-10 was purchased from Sigma–Aldrich. Bacterial and fungal isolates (p.a) of *S.aureus*, *E.coli*, *P. aeruginosa*, *C.*

albicans, and *A. fumigatus* were obtained from the microbial type culture collection, Microbiology Laboratory, Medical Faculty of Andalas University, West Sumatera, Indonesia.

2.2. Preparation of *M. oleifera* leaf extract: Leaves of *M. oleifera* were collected from the Balai Benih Induk Tanaman (Center for Mother Plant Seed) in Lubuk Minturun, Koto Tangah, Padang, West Sumatra, Indonesia. Taxonomic identification was carried out in Herbarium Universitas Andalas (ANDA), Andalas University, Padang, Indonesia. Secondary metabolites were identified at the Laboratory of Natural Products, Chemistry Department, Andalas University. The leaves were shade-dried at room temperature for about 5 days, and were then mashed up to obtain a fine powder. Ten grams of *M. oleifera* leaf powder was dissolved in 50 mL double distilled water for 30 min, at 65 °C. The obtained extract was filtered with Whatman No.1 filter paper, and was stored in a sealed bottle at a temperature of 4 °C for further use.

2.3. Green synthesis of cerium oxide nanoparticle (CeO_2NPs): A total of 3.72 g of cerium nitrate hexahydrate was added in 50 mL of *M. oleifera* leaf extract. The solution was stirred using a magnetic stirrer at 80 °C for 2 h, until the solution had changed color from dark brown to light brown. Resulting solid was calcined at 600 °C for 2 h, to obtain CeO_2NPs. Figure 1. Depicts a schematic diagram of the synthesis process of cerium oxide nanoparticles.

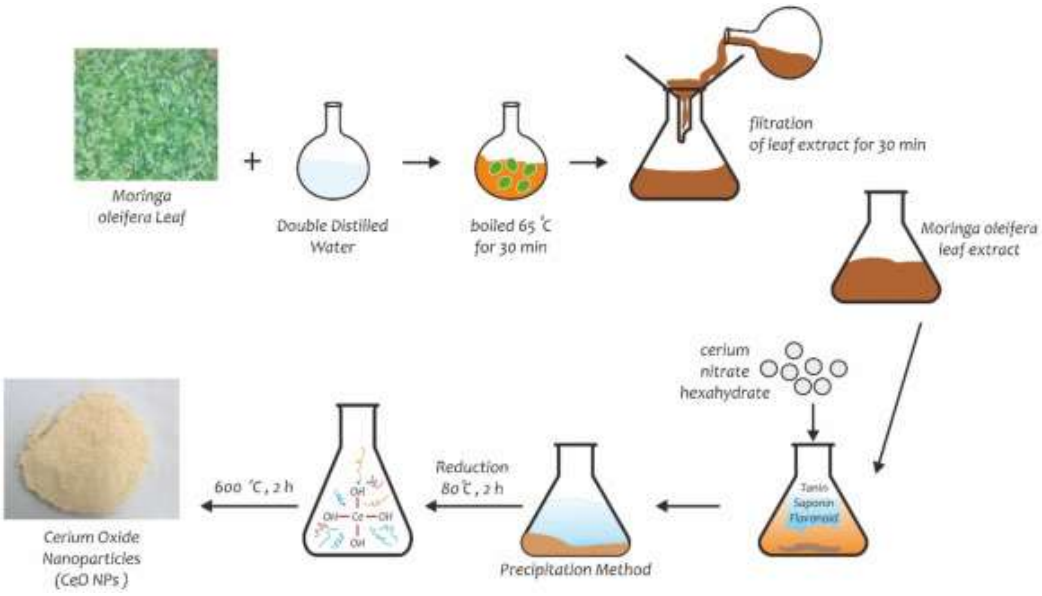

Fig. 1. Schematic diagram of CeO_2NPs synthesis process.

2.4. Characterization of cerium oxide nanoparticle (CeO_2NPs): The morphology of CeO_2NPs was analyzed using SEM (FEI, Inspect-S-50) operating at 20 kV and TEM (JEOL JEM 1400) operating at 120 kV. The optical properties of CeO_2NPs were analyzed using

a DRS UV–Vis (Spectron 210 Plus, Analyticjena) instrument. Functional groups contained in the sample were analyzed using PerkinElmer Frontier FT-IR (FTIR) in the 400-4000 cm^{-1} wavenumber range. Instrument XRD analysis was recorded using CuKα radiation (λ = 1.54060 Å). Xpert Pro Panalitycal PW 30/60 was used to characterize the crystallite structure of the samples with a nickel monochromator in the range of 2θ from 20° to 100°. The generator setting of the XRD instrument was set at 40 kV, 30 mA. To calculate the crystallite size of CeO_2NPs, Scherrer's equation was used.

2.5. Antimicrobial activity test: The antimicrobial activity test was conducted to determine the activity of CeO_2NPs against *S.aureus* as Gram positive (G+) bacteria, *E.coli* and *P. aeruginosa* as Gram negative (G-) bacteria, and *C. albicans* and *A. fumigatus* as fungi. All bacteria and fungi were cultured in sodium agar (NA) and Sabouraud Dextrose Agar (SDA), respectively, at a temperature of 37 °C, for 24 h. Each of the bacterial and fungi suspensions were added to 100 mL of NA and SDA media in Petri dish, respectively. Synthesized CeO_2NPs were dissolved in distilled water at various concentrations of 10, 50, and 100 mg/mL. As a negative control, 100 mg/mL of sterile distilled water was employed. The inhibition zone was measured after incubation in a visible-light irradiation reactor at 37 °C, for 24 h. This work was repeated in duplicate Results and Discussion.

3. Results and discussion

3.1. Cerium oxide nanoparticles formation: In this study, $Ce(NO_3)_3{\cdot}6H_2O$ as precursor was dissolved in three different solvents to test the solubility of the precursor, i.e., water, water with addition of base, and aqueous extract of *M. oleifera*. The results demonstrate that $Ce(NO_3)_3{\cdot}6H_2O$ dissolved efficiently in water. However, by the addition of a base, i.e., NH_4OH, a yellow precipitate was formed. In contrast, when added with an *M. oleifera* leaf aqueous extract, it formed a yellowish-brown solution with precipitates.

3.2. FTIR analysis: The FTIR spectrum of CeO_2NPs is presented. The FTIR analysis was conducted using the KBr pellet method, and was scanned in the 400-4000 cm^{-1} wavelength range. The FTIR spectrum of $CeNO_3.6H_2O$ shows the absorption band at 1030-1300 cm^{-1}, around 1600 cm^{-1}, and 3300 cm^{-1}, which are referred to as N–O stretching, H–O–H bond, and OH stretching, respectively. The FTIR absorption spectrum of CeO_2NPs before calcination shows the intensity of OH stretch and the N–O stretch of nitrate is still strong around 1300 cm^{-1}. Absorption peaks CeO_2NPs after calcination shows the appearance of a new peak of the Ce–O strain at a wavelength of 453 cm^{-1}, and a shift in the peak of the O–Ce–O bond 556 cm^{-1} with a stronger intensity and a decrease in the peak of NO stretching

nitrate is about 1030–1300 cm^{-1}. It was observed that the water OH peak appears to be reduced in the form of cerium oxide. The results of this study are in line with those by Arumugam et al., who also found the peak of Ce–O stretching to be 451 cm^{-1}.

3.3. SEM-EDX analysis: Analysis of SEM was conducted to characterize the morphology of the nanoparticle surface. as-prepared CeO_2NPs are spherical in shape with a uniform size but undergo agglomeration. Kannan et al. reported the synthesis of CeO_2NPs using leaf extract of *Acalypha indica*, in which agglomeration of the nanoparticles occurred as well. When the SEM image was enlarged, it was clearly pronounced. The SEM 2D elemental mapping of as-synthesized CeO_2NPs . It is clearly shown that atomic Ce and O are contained in the sample, without any other atom. In addition, EDX analysis results showed high intensity peaks of Ce and O in a specific energy of 20 keV. The absence of impurity in the EDX spectrum indicate the success of the CeO_2NPs synthesis process.

3.4. UV–Vis DRS analysis: The absorption and optical properties of the nanomaterial were investigated using UV–Vis DRS analysis. It is better than Ultraviolet (UV)-Visible Spectroscopy, due to the excess light scattering of powdered material, so it is unnecessary to dissolve the sample shown below. Shows the UV–Vis DRS absorption spectrum of CeO_2NPs. A high absorption intensity peak appears in the visible light region, with a wavelength of 352 nm. The band gap energy value of the green synthesized CeO_2NPs was determined by fitting absorption of direct transition with the following equation:(2)$\alpha h\upsilon = A(h\upsilon - E_g)^n$where the coefficient of optical absorption is α, the photon energy is (h.υ), the direct band gap is Eg, n = 2 and n = ½ are the values for the indirect and direct band gap, and A is a constant value . Based on the calculation of the formula, the value of the band gap energy was found to be 2.61 eV. The value is smaller than that possessed by the bulky sized CeO_2, which is 3.19 eV. This decrement in the band gap value is associated with quantum effects on nano scale particles.

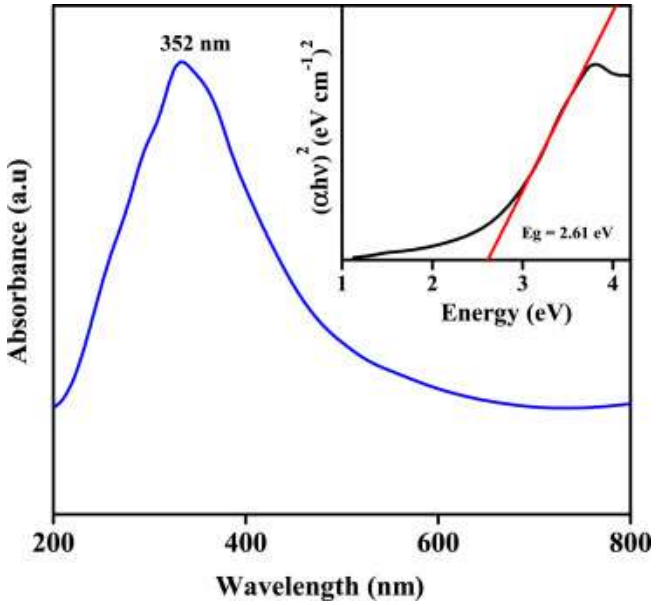

UV–Vis spectrum of as-synthesized CeO_2NPs sample. Inset demonstrates the touch plot for determination of band gap energy.

The difference of energy between the valence band (VB), which is dense with electrons, and the conduction band (CB), which is devoid of electrons, is called band gap energy. The energy value of the band gap in semiconductors is crucial due to its effect on the semiconductor's performance in flowing electrons and holes. The electrons jump from the VB to the non-free CB is caused by a small band gap energy., while a large one will inhibit their jump so it will block the flow of electrons . The energy value of the band gap of as-prepared CeO_2NPs is 2.61 eV. Sharma et al. green-synthesized CeO_2NPs by mediation of *Azadirachta indica* and found the band gap energy value to be 2.57 eV . Semiconductors are formed when the band gap energy is between 1 and 3 eV with a good ability to adsorb light in a visible region, hence, it has a good potential to be developed in biomedical applications.

3.5. Antimicrobial activity: Based on recent studies, cerium oxide nanoparticles have a potential to be applied as anti-microbial agent, because of their lower toxicity effects, heat resistance, and absorption effects in the UV–Vis region. The samples were tested against *Sida aureus*, *P. aeruginosa*, and *E. coli* bacteria. In addition, the antifungal activity was also tested against *C. albicans* and *A. fumigatus* fungi. The concentration of samples tested were 10, 50, and 100 mg/mL. The most significant result was obtained by the 100 mg/mL concentrated sample, in which the inhibition zone of CeO_2NPs antibacterial test against *S. aureus, P. aeruginosa* and *E. coli* bacteria was 22, 16, and 15 mm, respectively. The antifungal activity of the sample against *C. albicans* and *A. fumigatus* was shown by the inhibition zone of 20

and 26 mm, respectively. These results suggest that as-synthesized CeO_2NPs has a strong antimicrobial activity, as the inhibition zone value of 10–20 mm is classified as strong, while the inhibition zone of more than 20 mm is classified as very strong.

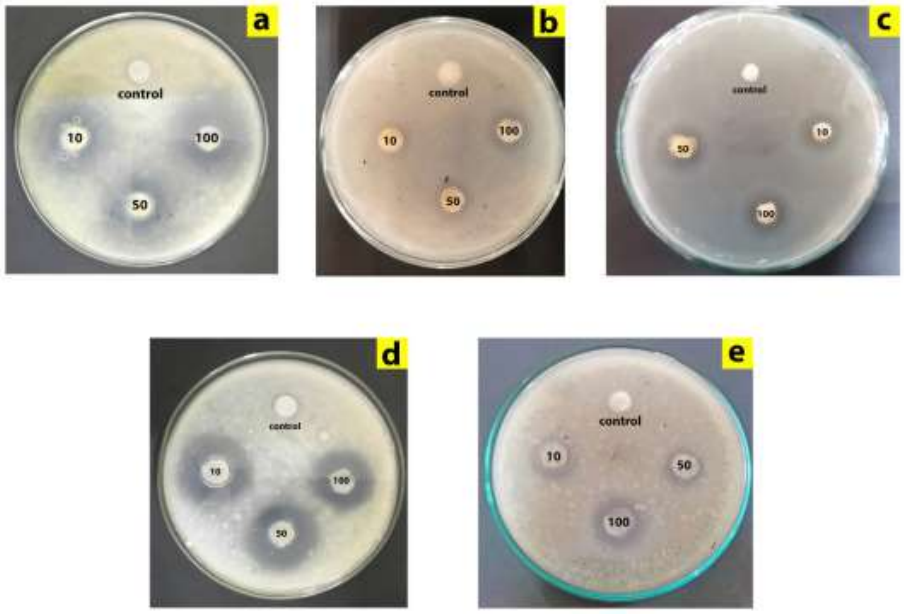

Inhibition zone of *Moringa oleifera* mediated synthesized CeO_2NPs against some bacteria (a) *S.aureus* (b) *E.coli* (c) *P.aeruginosa* and fungal (d) *A.fumigatus* (e) *C.albicans*.

Based, Gram-positive bacteria are more susceptible to CeO_2NPs compared to their Gram-negative counterparts. This might be due to the higher sensitivity of Gram-positive bacteria to ROS than Gram-negative, since the former type has a thinner cell wall with fewer peptidoglycan composition. Peptidoglycan consists of constituent compounds in the form of thiol group that is easy to interact with ROS. On the other hand, the cell wall of Gram-negative bacteria consists of a thick lipid layer.The antifungal properties of CeO_2NPs also showed better results than antibacterial properties, where the inhibition zone values are over 20 mm, which are classified as very strong.

Provides the inhibition zone of CeO_2NPs reported in some prominent studies, in which *M. oleifera* mediated synthesis of CeO_2NPs demonstrated a higher inhibition zone compared to the samples of those previous studies. In addition, different types of concentrations of CeO_2NPs cause differences in their antimicrobial properties.

The antibacterial properties of CeO_2NPs synthesized using *M. oleifera* leaf extract were better than the ones reported in previous studies. This is related to particle size based on TEM analysis results, in which it resulted in a smaller particle size (i.e., 17 nm). A smaller particles size leads to a larger specific surface area, hence provides more active sites to contact with the bacteria cells. Besides, the smaller sized-particles are easier to penetrate into

the bacteria cells, causing the cells to die. In addition, it is associated with photocatalytic activity, in which, based on DRS-UV analysis results, band gap energy value CeO_2NPs is of 2.61 eV. The semiconductor absorbs photons when exposed to light that is greater than or equal to the band gap energy. Hence, it enables the photocatalytic activity by producing radicals that can inactivate bacteria/micropollutants. The active antibacterial and photocatalytic properties of these CeO_2NPs can be developed in a wider field, both in biomedicine and industry, to decompose micropollutants in water by visible light irradiation.

The exact mechanism of the antifungal activity of CeO_2NPs has not yet been fully understood. However, antimicrobial potential may be largely due to electromagnetic interactions and ROS formation, such as the production of hydroxyl radicals (OH•) from CeO_2NPs around lipid membranes. ROS induces oxidative damage to cell membrane lipids , thus denaturing cell membrane permeability, ultimately leading to cell death . These high antifungal results indicate that CeO_2NPs has a high potential to be applied in the biomedical field. This might be due to the difficulty of finding antifungal compounds, since their eukaryotes have similarities at the biological level to human eukaryotic cells. Furthermore, further research on the development of antifungal drugs with less side effects merits further investigation.

Explains mechanism of antibacterial activity of CeO_2NPs with bacterial cell wall. CeO_2NPs are semiconductors. When exposed to light or photons with similar or exceeding energy value of band gap, the electrons are excited from the ground state (Valence band (VB)) to a higher energy level or excited state (Conduction band (CB)), and produce holes (h^+). The mechanism of reduction and oxidation through the formation of holes and electrons are utilized in a degradation process of bacteria that contacts the surface of the photocatalyst. Both electrons and holes have the ability to produce reactive ions, which can be used to deactivate and decompose pollutants or hazardous microbes. In this case, electrons react with air or oxygen (O_2) to make radicals of superoxide ($\cdot O_2^-$), while holes interact with water molecules (H_2O) to form active radicals of hydroxyl ($OH\cdot$) and H_2O^+ . The Reactive Oxygen Species (ROS) produced by CeO_2NPs i.e. $OH\cdot$ and $\cdot O_2^-$ enter the bacteria, which can affect cells. The reaction mechanism for the production of ROS by CeO_2NPs and is described hereafter.(3)$CeO_2 + h\upsilon \rightarrow e^- + h^+(4)h^+ + H_2O \rightarrow OH\cdot + H_2O^+$(5)e⁻+O2→·O2-

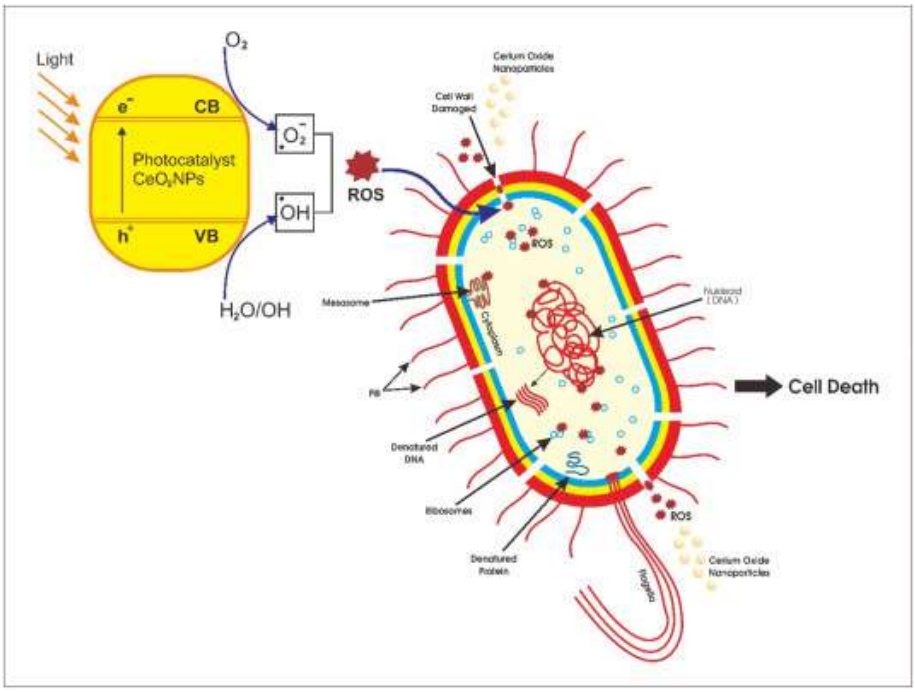

Mechanism of antibacterial activity of CeO_2NPs with bacterial cell wall, CeO_2NPs generates of reactive oxygen species (ROS) which affects ribosomes, proteins, cytoplasm and DNA. This mechanism ultimately leads to cell death.

The electrostatic interaction between the positively charged CeO_2NPs and the negatively charged bacterial cell surface is principally responsible for CeO_2NPs antibacterial activity. This condition is crucial for the activity of CeO_2NPs as a bactericidal agent . This antibacterial activity is due to the photocatalytic properties of the nanoparticles . After ROS enters bacterial cells, ROS interacts with cell components in bacteria, including the mesosome, cytoplasm, protein, and nucleoid, thus damaging the components, weakening the cells, and leading to their death . CeO_2NPs have strong antibacterial properties, since they produce higher ROS due to the large surface area and a small crystal size, as previously explained in the XRD analysis results section. However, in healthy human cells, the effect of nanoceria can serve as an antioxidant through the ROS scavenging process . This is a promising research direction that focuses on the biomedical application of CeO_2NPs as antioxidants.

4. Conclusions: CeO_2NPs were successfully synthesized using the aqueous extract of *M. oleifera* leaves, without the addition of acids or bases, and were synthesized in short reaction time of 5 h. XRD analysis revealed the formation of high crystallinity CeO_2 with a cubic structure. The as-synthesized CeO_2NPs were spherical in shape, with average particle size of 17 nm. Based on the EDX analysis, as-synthesized samples contained high purity cerium and oxygen without any impurities, proven by high intensity peaks. The resulting nanoparticles

have very effective antimicrobial activity, showing a high potential to be reliably applied in biomedical applications.

References

1.A. Arumugam, C. Karthikeyan, A.S. Haja Hameed, K. Gopinath, S. Gowri, V. Karthika Synthesis of cerium oxide nanoparticles using Gloriosa superba L. leaf extract and their structural, optical and antibacterial properties Mater Sci Eng C, 49 (2015), pp. 408-415, 10.1016/j.msec.2015.01.042

2. M. Bhagat, S. Rajput, S. Arya, S. Khan, P. Lehana Biological and electrical properties of biosynthesized silver nanoparticles Bull Mater Sci, 38 (2015), pp. 1253-1258, 10.1007/s12034-015-1007-8

3. S.K. Kannan, M. Sundrarajan A green approach for the synthesis of a cerium oxide nanoparticle: characterization and antibacterial activity Int J Nanosci, 13 (2014), pp. 1-7, 10.1142/S0219581X14500185

4. N. Thovhogi, A. Diallo, A. Gurib-Fakim, M. Maaza Nanoparticles green synthesis by Hibiscus Sabdariffa flower extract: main physical properties J Alloys Compd, 647 (2015), pp. 392-396, 10.1016/j.jallcom.2015.06.076

5. Q. Maqbool, M. Nazar, S. Naz, T. Hussain, N. Jabeen, R. Kausar, *et al.* Antimicrobial potential of green synthesized CeO2 nanoparticles from Olea europaea leaf extract Int J Nanomed, 11 (2016), pp. 5015-5025, 10.2147/IJN.S113508

6. N.K. Renuka Structural characteristics of quantum-size ceria nano particles synthesized via simple ammonia precipitation J Alloys Compd, 513 (2012), pp. 230-235, 10.1016/j.jallcom.2011.10.027

7. R. Suresh, V. Ponnuswamy, R. Mariappan Effect of annealing temperature on the microstructural, optical and electrical properties of CeO 2 nanoparticles by chemical precipitation method Appl Surf Sci, 273 (2013), pp. 457-464, 10.1016/j.apsusc.2013.02.062

8. S. Habtemariam, G.K. Varghese Extractability of rutin in herbal tea preparations of moringa stenopetala leaves Beverages, 1 (2015), pp. 169-182, 10.3390/beverages1030169

9. B. Vongsak, P. Sithisarn, W. Gritsanapan Bioactive contents and free radical scavenging activity of Moringa oleifera leaf extract under different storage conditions Ind Crop Prod, 49 (2013), pp. 419-421, 10.1016/j.indcrop.2013.05.018

10. M. Darroudi, S.J. Hoseini, R. Kazemi Oskuee, H.A. Hosseini, L. Gholami, S. Gerayli Food-directed synthesis of cerium oxide nanoparticles and their neurotoxicity effects Ceram Int, 40 (2014), pp. 7425-7430, 10.1016/j.ceramint.2013.12.089
11. V. Morris, P.G. Fleming, J.D. Holmes, M.A. Morris Comparison of the preparation of cerium oxide nanocrystallites by forward (base to acid) and reverse (acid to base) precipitation Chem Eng Sci, 91 (2013), pp. 102-110, 10.1016/j.ces.2013.01.016
12. A. R. Unnithan, A. Ramachandra Kurup Sasikala, Y. Sathishkumar, Y.S. Lee, C.H. Park, C.S. Kim Nanoceria doped electrospun antibacterial composite mats for potential biomedical applicationsCeram Int, 40 (2014), pp. 12003-12012, 10.1016/j.ceramint.2014.04.038